



# Explainable Artificial Intelligence for deriving 3D dynamic rainfall thresholds for landslide triggering using Kolmogorov-Arnold Networks

Lukas Schild<sup>1</sup>, Ascanio Rosi<sup>2</sup>, and Filippo Catani<sup>2</sup>

<sup>1</sup>Department of Civil Engineering and Environmental Science, Western Norway University of Applied Sciences, Norway

<sup>2</sup>Department of Geosciences, University of Padova, Italy

**Correspondence:** Lukas Schild ([lukas.schild@hvl.no](mailto:lukas.schild@hvl.no))

**Abstract.** Landslides triggered by rainfall are a significant hazard in mountainous regions worldwide, posing risks to both infrastructure and human safety. Projections regarding climate change indicate an increase in both extreme weather events and subsequent landslide incidents. Therefore, accurately forecasting these rainfall-induced landslides is essential for implementing effective hazard mitigation and evacuation strategies. Traditionally, predictions have relied on physically based models and empirical rainfall thresholds that account for both rainfall intensity and duration. With the introduction of Machine Learning, the ability to incorporate static factors—such as slope gradients and soil classifications—has been significantly improved, thereby enhancing predictive accuracy and enabling broader spatial applications. Nonetheless, recent research involving Machine Learning has predominantly concentrated on established deep learning frameworks, while innovative approaches have not been thoroughly investigated. This hesitance to embrace contemporary deep learning techniques may stem from challenges in interpreting the decisions made by these models, which are vital for effective operational landslide early warning systems. Recent studies emphasising traditional Machine Learning frequently include analyses of network behaviour through post-hoc interpretations, utilising methods such as Shapley values and assessments of feature importance. However, the use of inherently explainable deep learning networks for rainfall-induced landslide prediction remains underexplored. To address this gap, we propose employing Kolmogorov-Arnold Networks (KANs) to predict rainfall-induced landslides, leveraging precipitation time series obtained from a globally accessible satellite product. The proposed model achieves competitive performance compared to various established models while maintaining interpretability. In addition to utilising interpretable activation functions, we also suggest implementing Dynamic Rainfall Thresholds (DRT) as a visual interpretation tool for the model. This combination of interpretative tools, paired with a low rate of missed alarms, positions the model as a suitable option for critical applications such as landslide early warning systems.

## 20 1 Introduction

Landslides globally constitute a major hazard in mountainous regions, threatening communities and infrastructure in their vicinities. Moreover, climate change scenarios suggest an increase in extreme weather events and related landslide occurrences (Jemec Aulfič et al., 2023; Gariano and Guzzetti, 2016). Thus, efficient and accurate early warnings systems are indispensable



tools for civil protection along with other mitigation measures. In this context, different approaches to predicting landslides  
25 have been investigated. Physically based models and empirical thresholds based on intensity and duration of rainfall events are  
commonly employed to assess landslide risk and issue warnings (Berti et al., 2012; Brunetti et al., 2010; Piciullo et al., 2017).  
More recent advances in landslide prediction leverage Machine Learning techniques, such as Artificial Neural Networks,  
to consider static predisposing factors in addition to, for example, precipitation time series. These machine learning based  
models generally outperform conventional empirical-statistical methods regarding landslide prediction accuracy (Dal Seno  
30 et al., 2024). Predisposing factors, such as slope angles, soil types and historic rainfall data, might however not be available  
for all landslide risk zones. Thus, efforts focusing on leveraging the connection between previously observed landslides and  
precipitation records have shown promising results employing machine learning (Mondini et al., 2023; Nocentini et al., 2023).  
However, these studies rely on established (deep) learning architectures, such as Multilayer Perceptrons (MLPs) and Decision  
Tree based methods, and are not leveraging the most recent advances in the field of machine learning (Tehrani et al., 2022).  
35 A possible explanation could be found in the inherent difficulty of interpreting large state-of-the-art machine learning models.  
This lack of interpretability constitutes a major hurdle for machine learning systems to be adapted in practice as their decisions  
must be well understood (Dal Seno et al., 2024; Gu and Dao, 2024; Zhang and Yan, 2023). Recent studies have attempted  
to employ post-hoc explanations, for example the game-theory based Shapley values, to understand the effect of the various  
inputs on the output of the optimised model after training (Wen et al., 2025). However, Shapley values can be computationally  
40 expensive as they are sample based and supply only local and often hard to interpret explanation even with a large number of  
samples. Other studies add feature importances or Partial Dependence Plots to complete the image of the model behaviour and  
to understand the underlying data generating process and even derive rainfall thresholds (Franceschini et al., 2025; Nocentini  
et al., 2023). While rendering the model globally more transparent, feature importances only show the weight of the inputs  
on the output but not their inferred relation. To this end, we propose the use of Kolmogorov-Arnold Networks (KANs) in  
45 the context of landslide prediction tasks (Liu et al., 2024). KANs provide competitive performance on small datasets through  
learning inherently interpretable activation functions, rather than weight matrices in an MLP with fixed activation functions.  
Furthermore, their effectiveness on a variety of problems such as time series regression, concept drift detection, graph learning  
and vision tasks has been documented (Han et al., 2024; Xu et al., 2024; Bresson et al., 2024; Cheon, 2024). To address the  
issues of data availability and model interpretation from a practical point of view, we propose the use of KANs to predict  
50 rainfall induces Shallow Landslides based on precipitation time series derived from a globally available satellite product. The  
presented model is compared to frequently employed Random Forest based models (Breiman, 2001), Tree Gradient Boosting  
with XGBoost (Chen and Guestrin, 2016) and Multilayer Perceptrons (MLPs) and exhibits competitive performance, especially  
regarding the classification of positive samples. In addition to an examination of the learnt activation functions, we propose  
the computation and visualisation of Dynamic Rainfall Thresholds (DRTs) to interpret the model decisions and showcase  
55 the practical application of the model and the DRT based explanation in an Early Warning system. Leveraging the inherent  
interpretability of KAN based models together with the innovative DRT visualisation enables the usage of modern state-of-  
the-art machine learning for critical application tasks, such as in landslide Early Warning Systems. This approach gives crucial



insights into the relations machine learning models extract from datasets beyond the presented application, enabling deeper understanding of the underlying data generating processes.

## 60 2 Methodology

In order to train machine learning based model for the task of predicting Shallow Landslides, we constructed a dataset consisting of historical precipitation records and landslide occurrences. In addition to the antecedent rainfall in the 30 days prior to the prediction date, we add the day of the year as an input variable to encode seasonal dependencies (Rosi, 2023). The compiled dataset is then used to train a range of Machine Learning models with the aim to predict two classes, *failure* and *non-failure* based on the input sequence. The dataset set is split into training (90% of data) and test (10% of data) to train the model and assess model performance during and after training. Furthermore, a total of 40 randomly selected rainfall events (20 failure events, 20 non-failure events) have been withheld from the dataset, to use as validation set and to showcase the application of the model for spatio-temporal forecasting. Lastly, to enhance the model interpretability, we derive sample dependent Dynamic Rainfall Thresholds (DRTs) from the activation functions of a KAN based machine learning model.

### 70 2.1 Dataset Preparation

We construct a dataset consisting of the antecedent cumulated rainfall from one day to 30 days prior to the prediction date in one day increments (*precip\_1d* to *precip\_30d*), the day of the year of the prediction date *doy* and whether or not a failure occurred on the prediction date (*fail*) (Tab 1).

The antecedent rainfall data is based on precipitation time series from Global Precipitation Measurements (GPM) acquired

**Table 1.** Dataset variables

Variable	Description	Data Type
<i>doy</i>	day of the year	Integer
<i>precip_xd</i>	daily cumulated precipitation <i>x</i> days before prediction date; $x \in [1; 30]$	Integer
<i>fail</i>	failure occurrence for prediction date	Boolean (true/false)

75 through Integrated Multi-satellitE Retrievals for GPM (IMERG) (Huffman et al., 2015). This open source product provides half-hourly cumulated precipitation measurements for most locations in the world. The measurements are combined based on measurements from a range of satellite instruments. This study used the *Final Run* product as provided by the United States National Space Agency (NASA). The final run product contains corrected measurements, where ground-based rain gauges have been used to correct the gridded rainfall data that is provided in  $0.1^\circ$  by  $0.1^\circ$  grid cells.

80 The e-ITALICA landslide inventory has been used as a base for data regarding rainfall induced landslide events between 1996



and 2021 (Brunetti et al., 2025). From the inventory we extract date and time for all Shallow Landslides in Northern Italy (above 44° North) to use as positive samples in the dataset (Fig. 1). Although the inventory provides records on different types of failures in Northern Italy, including Earth Flows (89 events), Debris Flows (146), Mud Flows (56) and Rock Falls (337 events), the relatively large number of recorded Shallow Landslides (2022 events) makes this failure type the most suitable for machine learning based predictions. Furthermore, focusing on one particular failure type is beneficial for model performance as well as interpreting the model behaviour when compared to datasets with mixed landslide types (Segoni et al., 2018a).

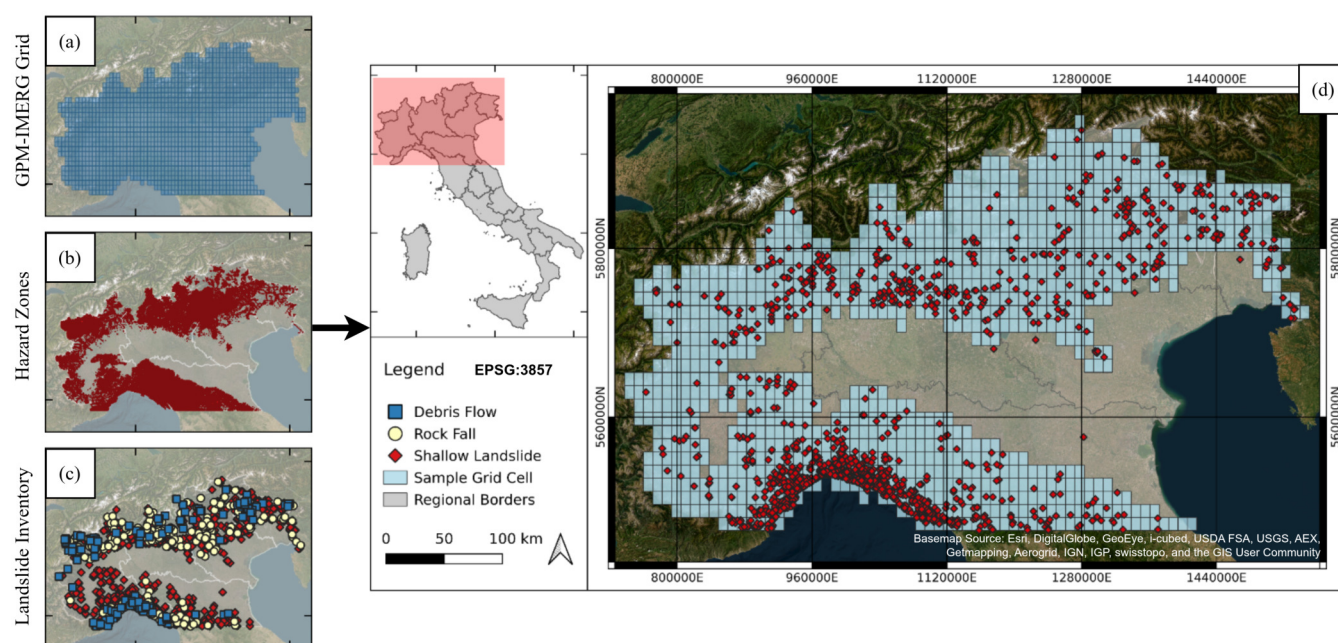


**Figure 1.** Dataset construction using (a) GPM-IMERG Grid Cells, (b) Landslide Hazard Zones as defined by the Italian Institute for Environmental Protection and Research (ISPRA) and (c) the e-ITALICA landslide inventory.

The final classification dataset contains  $\approx 20,000$  dates (rainfall events) where no Shallow Landslide has been recorded in the given grid cell and 2022 failure events, forming a highly imbalanced dataset ( $\approx 1/10$  ratio failure/non-failure). Samples have accordingly been generated to spread uniformly across the temporal and spatial domain. The temporal domain ranges from 01.01.1996 to 31.12.2021 in accordance with the time span documented in the e-ITALICA dataset and samples have been drawn for any of the 24 hours of the day. Landslide occurrence dates from e-ITALICA have been rounded to the nearest hour, regardless of their temporal accuracy as antecedent rainfall is only captured with a daily resolution. The spatial domain contains all  $0.1^\circ$  by  $0.1^\circ$  GPM-IMERG grid cells (Fig. 1 a) that intersect with the Italian borders as well as landslide hazard zones as defined by the Italian Institute for Environmental Protection and Research (ISPRA) (Fig. 1 b).



## 95 2.2 Network Explanations

The KAN models trained and evaluated in this study have been implemented using the Python package *pykan* (Liu et al., 2024). KANs are named after the Kolmogorov-Arnold representation theorem which states that composition of a finite number of one-dimensional functions can represent high-dimensional functions. Based on this theorem, KAN layers learn activation functions and the output of the layer is summed before the next activation function is applied. The activation functions of a KAN layer are combinations of spline functions with a single parameter. Note that we use a standard architecture with a single neuron in the output layer for the MLP as this architecture is most commonly used for classification tasks with only two classes. At the same time we train and evaluate KAN networks with *two* outputs, one per class. This allows for a simpler computation of the proposed Dynamic Rainfall Threshold which directly used the combinations of activation functions used to predict failure, i.e. on the path from all inputs to the failure output and those on the path to the non-failure output.

105 After training the KAN model, a visualization of the activation functions aids in interpreting how different input values affect the activation of each of the neurons in the network. The shallower the network, i.e. the lower the number of layers, the easier these generally are to interpret. Combining interpretation of the activation functions and feature importance scores provides a comprehensive explanation of the network behaviour (Lundberg and Lee, 2017).

Besides the explanations provided by inspecting the learnt activation functions and feature importance scores, the nature of KANs allows for a further explanation strategy, herein called Dynamic Rainfall Thresholds (DRT). DRTs can be derived from the learnt activation functions by fitting the activation functions to a symbolic prototype function. The prototype function is chosen from a list of base functions as the closest fit and subsequently refined to minimize a fitting error. The result is one symbolic function per activation function, where the precision of the fitted parameter can be refined to machine precision. This representation as a symbolic function introduces a loss in prediction accuracy compared to the original sum of parametrized spline base functions and is thus not suitable for prediction tasks. However, the symbolization of the activation function allows for a visual representation of the decision boundary the network learnt during training. This boundary can be found as the equilibrium point between the function predicting the failure output and the function predicting the non-failure output (Fig. 2). We utilize the antecedent rainfall in the three days prior to the event to compute the boundary, allowing the visualization as a three-dimensional decision boundary. Because the threshold visualization depends on the values of a specific sample, we adapt the naming of a Dynamic Threshold, as opposed to static 3D rainfall thresholds (Rosi et al., 2021).

120 All results presented have been computed using the `pytorch` and `pykan` packages with Python 3.11.4 on a Laptop with a 16 core AMD Ryzen 9 6900hx processor with 32GB memory and an NVIDIA GeForce GTX 3070 Ti Graphic Processing Unit (GPU) with 8GB memory using CUDA 12.7.

## 3 Results

125 We consider the binary classification case where all shallow landslide types are labelled "failure" as the positive class and non-failure events are the negative class. Because accuracy alone is not capturing how well the classifier can distinguish between two imbalanced classes, we report the Area Under the Receiver Operating Curve (ROC-AUC), representing how likely the

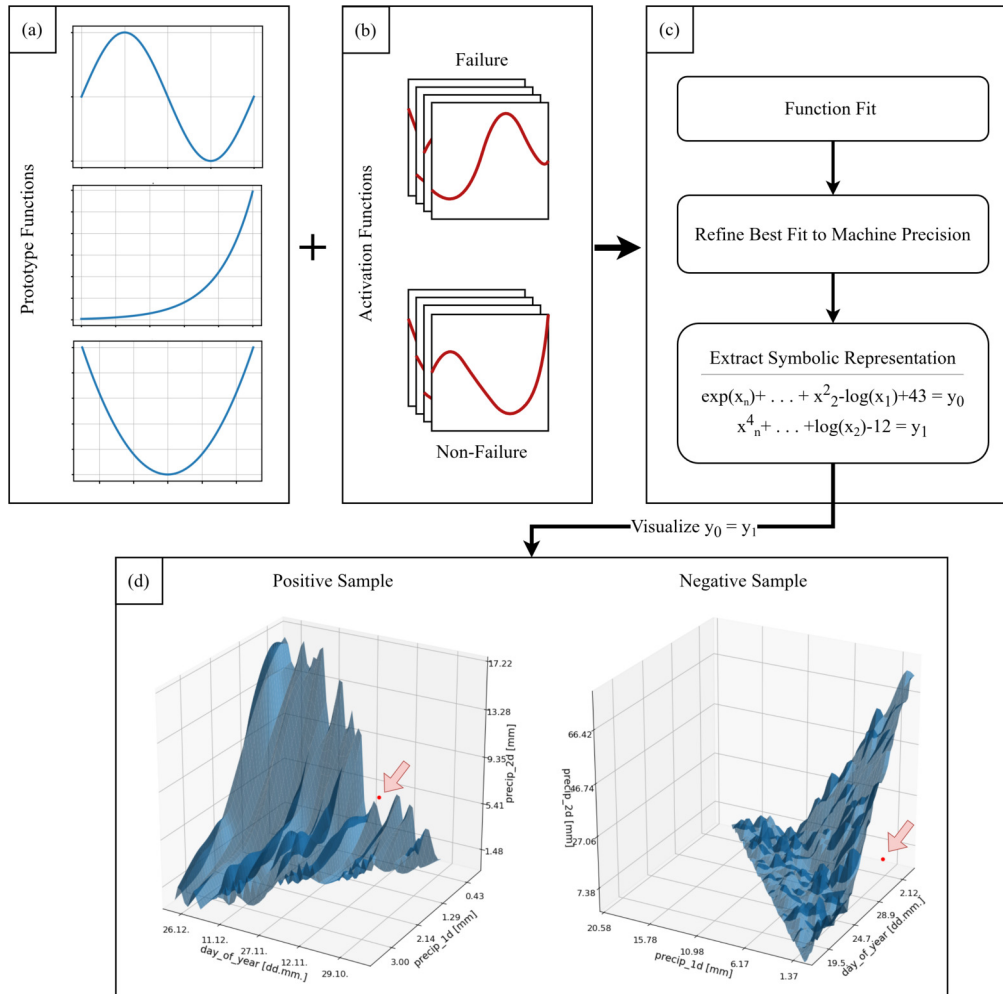


**Figure 2.** Dynamic Rainfall Threshold derivation using (a) a set of predefined prototype functions and (b) learnt activation functions of a Kolmogorov-Arnold Network to (c) find a symbolic representation of how the input is mapped to the output of the network. The boundary of the class "decision" can be visualised (d).

given model will attribute a higher probability to the positive class given a random positive and negative sample. Additionally, we report the True Skill Statistic (TSS), which is taking into account omission and commission errors and is not affected by prevalence nor the size of the test set (eq. 1) (Allouche et al., 2006). The TSS combines in one score the *True Positive Rate* (TPR), fraction of all true positives that were classified correctly, and *False Positive Rate* (FPR), the fraction of incorrectly classified true negatives, i.e. false alarms.



**Table 2.** Model metric comparison for prediction of the binary class *Failure/No Failure* on the test set with 2650 *No Failure* samples and 172 *Failure* samples.

Model	ROC-AUC	Accuracy	True Positive Rate (TPR)	False Positive Rate (FPR)	TSS
Random Forest	0.919	0.960	0.541	0.013	0.528
XGBoost	0.926	0.961	0.523	0.011	0.512
MLP	0.882	0.949	0.546	0.025	0.522
KAN	0.850	0.866	0.837	0.133	0.704

$$\text{True Skill Statistic} = \frac{TP}{TP + FN} - \frac{FP}{FP + TN} = TPR - FPR \quad (1)$$

While decision tree based methods and MLPs are exhibiting high accuracy values (95%), their TSS is weak compared to our KAN based model (MLP  $\approx$  0.54; KAN  $\approx$  0.7). This indicates that the base models are frequently missing alarms (MLP  $\approx$  46%; KAN  $\approx$  17%) while KAN based models more often predict false alarms (MLP  $\approx$  2%; KAN  $\approx$  13%). This leads to the KAN model having lower overall accuracy ( $\approx$  86%) as it more frequently misclassifies negative samples (Tab. 2).

### 3.1 Validation

For comparability with similar studies, in particular (Mondini et al., 2023), we illustrate the KAN model performance on a set of 40 randomly selected validation rainfall events, 20 rainfall events with landslides and 20 without landslides. The samples have been withheld from the training and testing sets used above. The model achieves on average an  $F_1$  score of  $F_1 \approx 0.9$  and Cohen's kappa of  $\kappa \approx 0.8$  on the validation set with two misclassified failure events and two misclassified non-failure events. The validation set performance has been evaluated as an average of 10 different validation sets and accordingly separate trainings in order to achieve a representative prediction performance. Misclassified positive samples tend to be in the Liguria region where also most failure related events in the dataset have been recorded (Fig. 3, representative validation set).

The activation functions of the KAN model can be inspected after training. The model used to generate the results consists of two layers, making it feasible to inspect all  $34 \times 2$  ( $no\_inputs \times no\_outputs$ ) activation functions of the model. Together with feature importance scores, the activation functions can be ranked and the most important ones visualised to support model interpretation. Figure 3 illustrates the activation functions of the four most important features for the model. The activation functions that receive precipitation amounts closer to the prediction date tend to have steeper rising activation functions for the positive class. The activation functions receiving the day of the year have more characteristic shapes showing that the model captured the temporal distribution of Shallow Landslide events, which are more frequently present in the dataset during autumn (Fig. 3).

Furthermore, the Dynamic Rainfall Thresholds can be visualised for specific samples, as for example misclassified samples from the validation set. The activation functions have been fitted with prototype functions using an acceptance fit threshold

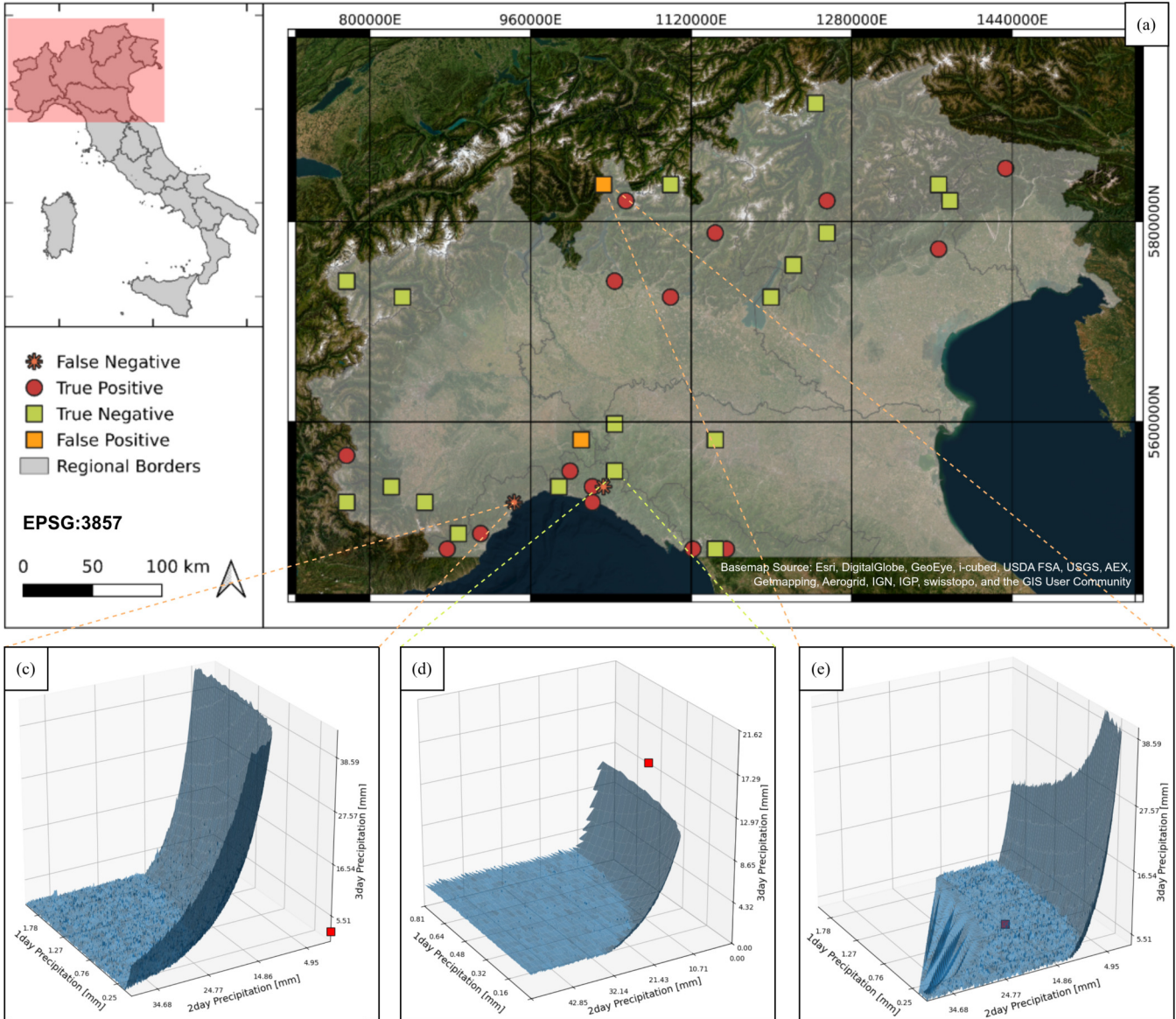


**Figure 3.** Map over Northern Italy with randomly selected Validation Data (a) with the activation functions of the KAN network that produced the predictions (b). The misclassifications are explained for one False Negative (c), one True Positive (d) and one False Positive (e) using the Dynamic Thresholds based on the precipitation of the three days prior to the prediction date.

of 95%. The resulting symbolic function for the two outputs performs less well on both test ( $\Delta acc \approx +4\%$ ,  $\Delta TSS \approx -0.08$ ) and validation set ( $\Delta F_1 \approx -0.03$ ,  $\Delta \kappa \approx -0.05$ ). The DRT visualisation is based on the three most important features based on their feature importance scores (2-days antecedent rainfall, 3-days antecedent rainfall and 1-day antecedent rainfall, Fig. 4).



Visualising the DRT for wrongly classified samples reveals for which variable combinations the values present in the samples

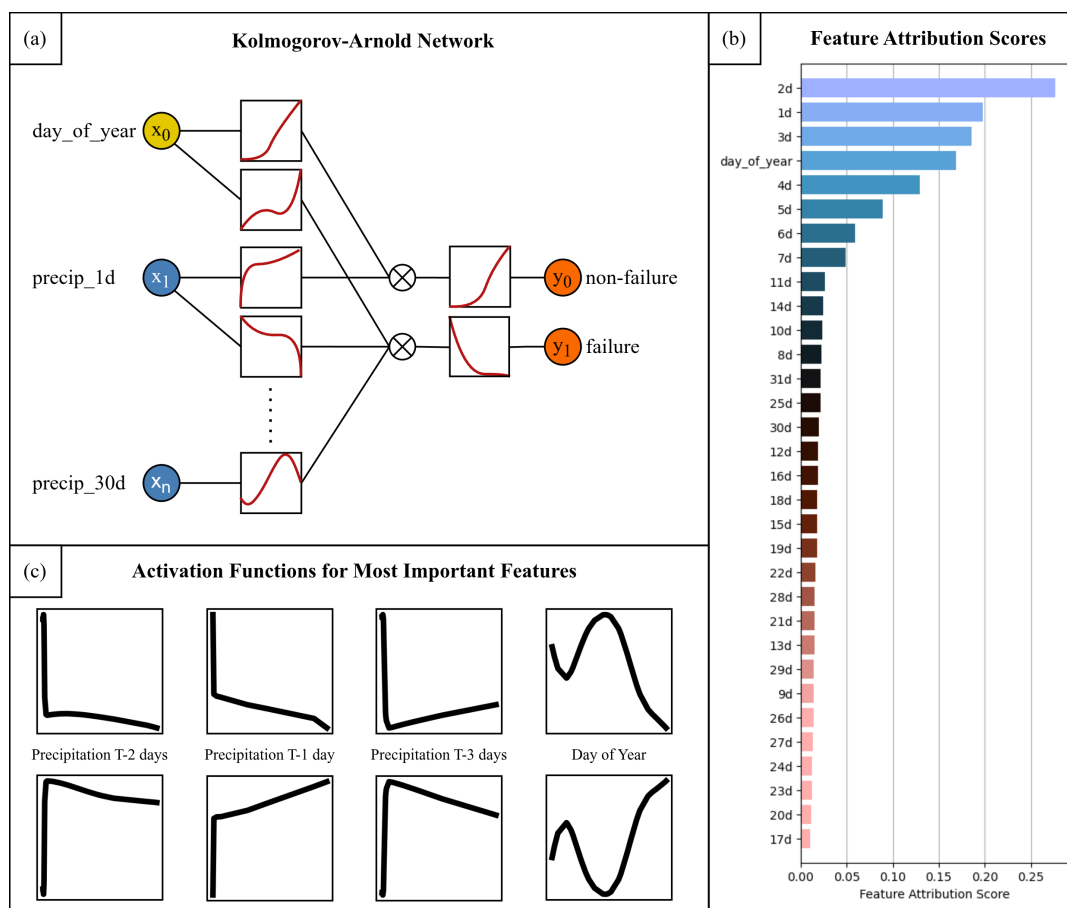


**Figure 4.** Kolmogorov Arnold Network with two outputs (a) and feature importances after training (b). The most important activation functions for both outputs (*non-failure* class top; *failure* class bottom) visualised according to their attribution scores (c).

160

were below the Dynamic Thresholds (Fig. 3 c-e). The variables not present in the plot influence the position of the surface, resulting in a similar shape but shifted position for the inspected DRTs. The two misclassified failure events were both preceded by very low precipitation amounts in the days prior to the event, resulting in the sample being below the failure threshold (Fig. 3 c,d). One of the misclassified non-failure events had been preceded by a high precipitation amount two days prior to the event, resulting in the sample laying close to but above the threshold (Fig. 3 e).

165



#### 4 Discussion

In the context of an Early Warning System for rainfall induced Shallow Landslides, the correct classification of positive samples, i.e. rainfall events that lead to failures, prevails the correct classification of negative samples. Nonetheless, an ideal model would achieve high accuracy for both positive and negative samples to reduce the number of false and missed alarms (Nocentini et al., 2023). Our comparison of commonly used Machine Learning models with KAN networks shows that the inherent interpretability of KAN based networks does not imply lower accuracy in the case of a heavily imbalanced dataset where the correct classification of positive samples has the highest priority. With this focus, the presented model outperforms state-of-the-art machine learning approaches with regards to the True Skill Score while the reported scores for traditional models align with previously reported scores for MLPs and decision tree based models for precipitation based landslide prediction (Distefano et al., 2023).

Short-term rainfall as well as the *day of the year* feature have the biggest influence on the event classification. This finding is in line with similar studies and is intrinsically linked to a necessary build-up of pore-water pressure (Nocentini et al., 2023). The high importance of *day of the year* can be explained by the temporal distribution of the landslides in the inventory used to build the dataset. Here, much higher landslide occurrence has been recorded in autumn, coinciding with longer periods of heavier rainfall (Brunetti et al., 2025). While this feature has been used in other studies to improve prediction performance or better defined thresholds, we find that the activation function learnt for *day of the year* does not accurately represent the cyclic dependency of the input. The activation function encodes higher activations for days early in the year, whereas days late in the year have lower activation functions, despite the days being extremely close to each other (Fig. 3 b). Although this mismatch of activation is likely due to artifacts at the edge of the defined grid for the activation function, a different encoding of the temporal component, such as month of the event could be beneficial for the model performance.

The data used in this study has been derived from the globally available satellite product GPM-IMERG, making the method widely applicable as long as landslide inventory data is available for a given region. Additional features could be considered, such as remotely sensed soil moisture, which is intrinsically linked to landslide occurrence (Distefano et al., 2023; Segoni et al., 2018b; Zhao et al., 2025). However, more features might render the model less interpretable, demanding a trade-off between number of input features and interpretability. This could be partly counteracted by reducing the input features after some pre-training to a subset of the original features based on feature importance scores. Furthermore, higher resolution measurements might benefit the model performance, although at higher computational cost. Higher spatial resolution for precipitation measurements could be especially beneficial in highly variable areas where many slope units in various directions are under the same grid cell, i.e. in the Liguria region.

The complexity and thus interpretability of the activation functions is guided by the number of grid points for the function and the complexity of the base spline. While higher order splines may be beneficial for higher accuracy, lower order splines ( $k \in [2, 3, 4]$ ) may be sufficient in combination with a low number of grid points ( $grid \in [4, 6, 8]$ ). This is in line with general recommendations for KAN model training, where low complexity functions in combination with few and shallow layers can achieve good performance results. This is in stark contrast to general recommendations for dense layer networks (MLPs) which



200 tend to require deep and wide networks to achieve similar performance, sacrificing interpretability (Liu et al., 2024).  
Fitting a symbolic representation to the activation functions results in a significant loss of prediction accuracy. However, the  
presented DRTs that are based on the symbolic representations are not used to generate predictions but rather to aid in explain-  
ing the model predictions. They should be used in combination with domain knowledge and the visualisation of the activation  
functions themselves. As presented, the 3D-thresholds are based on the three most important features according to feature im-  
205 portance scores. The latter might be subject to change between model training and evaluation cycles as the model initialisations  
and training are guided by stochastic processes. Albeit infeasible, a holistic evaluation of DRTs for all feature combinations  
could provide the best explanation of the model prediction.

Furthermore, the KAN models employed in this study exclusively use the proposed standard implementation of KAN networks  
with B-splines (Liu et al., 2024). By basing our work on this implementation we aim to enhance reproducibility of our results.  
210 Nonetheless, different KAN implementations are available, mainly differing in functions used as base splines, such as Wavelets  
and Fourier Series (Bozorgasl and Chen, 2024; Zhang et al., 2025). Future improvements in KAN optimisation may further  
enhance interpretability.

Lastly, a combination of the presented approach with existing rainfall thresholds based on Intensity-Duration relations could  
further enhance the predictive capabilities of the model while adding an additional interpretation tool in the form of a differently  
215 derived threshold. The grid-cell based thresholds as presented can further be easily combined with Early Warning Systems that  
operate on sub-regional scale, with spatially confined thresholds (Segoni et al., 2025).

## 5 Conclusions

We present a novel approach to predicting Shallow Landslides based on a globally available remote sensing data for precipita-  
tion and Kolmogorov-Arnold Networks. We show that the inherent interpretability of Kolmogorov-Arnold Networks does not  
220 come with a trade-off with regards to prediction performance. Indeed, shallow and narrow networks, i.e. with few neurons and  
few layers, outperform large Multi-Layer Perceptrons and decision tree based networks, achieving significantly fewer missed  
alarms with a similar level of false alarms. At the same time, the activation functions of the model paired with the presented  
Dynamic Rainfall Thresholds provide unprecedented insights into the model behaviour. Future improvements in KAN model  
training, especially regarding the available spline functions, may further improve their predictive performance. Additionally,  
225 pairing DRTs with critical evaluation of the model predictions based on domain knowledge and comparison with traditional  
statistical rainfall thresholds can provide additional insights. This direction of research is promising to improve existing Early  
Warning Systems for rainfall induced landslides, aiding landslide hazard mitigation and reducing the number of fatalities.

*Code and data availability.* The code used to produce the results has been published in the GitHub repository associated with this publi-  
cation ([https://github.com/luuuuk/Dynamic\\_Rainfall\\_Thresholds](https://github.com/luuuuk/Dynamic_Rainfall_Thresholds)). Precipitation data has been provided by NASA, the derived dataset with  
230  $\approx 20,000$  samples as used in the publication is provided with the repository.

<https://doi.org/10.5194/egusphere-2026-1796>

Preprint. Discussion started: 18 May 2026

© Author(s) 2026. CC BY 4.0 License.



*Author contributions.* LS prepared data, implemented framework, conducted experiments, prepared manuscript; AR framework formulation, manuscript revision; FC framework formulation, manuscript revision.

*Competing interests.* At least one of the (co-)authors is a member of the editorial board of Natural Hazards and Earth System Sciences.

*Acknowledgements.* This work was supported by the "The Geosciences for Sustainable Development" project (Budget Ministero dell'Università e della Ricerca–Dipartimenti di Eccellenza 2023–2027 C93C23002690001)

235



## References

- Allouche, O., Tsoar, A., and Kadmon, R.: Assessing the accuracy of species distribution models: prevalence, kappa and the true skill statistic (TSS), *Journal of Applied Ecology*, 43, 1223–1232, <https://doi.org/https://doi.org/10.1111/j.1365-2664.2006.01214.x>, 2006.
- Berti, M., Martina, M. L. V., Franceschini, S., Pignone, S., Simoni, A., and Pizziolo, M.: Probabilistic rainfall thresholds for landslide occurrence using a Bayesian approach, *Journal of Geophysical Research: Earth Surface*, 117, <https://doi.org/https://doi.org/10.1029/2012JF002367>, 2012.
- Bozorgasl, Z. and Chen, H.: Wav-KAN: Wavelet Kolmogorov-Arnold Networks, <https://arxiv.org/abs/2405.12832>, 2024.
- Breiman, L.: Random Forests, *Machine Learning*, 45, 5–32, <https://doi.org/10.1023/A:1010933404324>, 2001.
- Bresson, R., Nikolentzos, G., Panagopoulos, G., Chatzianastasis, M., Pang, J., and Vazirgiannis, M.: KAGNNs: Kolmogorov-Arnold Networks meet Graph Learning, <https://arxiv.org/abs/2406.18380>, 2024.
- Brunetti, M. T., Peruccacci, S., Rossi, M., Luciani, S., Valigi, D., and Guzzetti, F.: Rainfall thresholds for the possible occurrence of landslides in Italy, *Natural Hazards and Earth System Sciences*, 10, 447–458, <https://doi.org/10.5194/nhess-10-447-2010>, 2010.
- Brunetti, M. T., Gariano, S. L., Melillo, M., Rossi, M., and Peruccacci, S.: An enhanced rainfall-induced landslide catalogue in Italy, *Scientific Data*, 12, 216, <https://doi.org/10.1038/s41597-025-04551-6>, 2025.
- Chen, T. and Guestrin, C.: XGBoost: A Scalable Tree Boosting System, in: *Proceedings of the 22nd ACM SIGKDD International Conference on Knowledge Discovery and Data Mining, KDD '16*, pp. 785–794, ACM, <https://doi.org/10.1145/2939672.2939785>, 2016.
- Cheon, M.: Demonstrating the Efficacy of Kolmogorov-Arnold Networks in Vision Tasks, <https://arxiv.org/abs/2406.14916>, 2024.
- Dal Seno, N., Evangelista, D., Piccolomini, E., and Berti, M.: Comparative analysis of conventional and machine learning techniques for rainfall threshold evaluation under complex geological conditions, *Landslides*, <https://doi.org/10.1007/s10346-024-02336-3>, 2024.
- Distefano, P., Peres, D. J., Piciullo, L., Palazzolo, N., Scandura, P., and Cancelliere, A.: Hydro-meteorological landslide triggering thresholds based on artificial neural networks using observed precipitation and ERA5-Land soil moisture, *Landslides*, 20, 2725–2739, <https://doi.org/10.1007/s10346-023-02132-5>, 2023.
- Franceschini, R., Nocentini, N., Rosi, A., Tunini, L., Zuliani, D., Peressi, G., and Rossi, G.: Deriving rainfall thresholds with XAI and GNSS measurements for a large landslide, *Landslides*, <https://doi.org/10.1007/s10346-025-02657-x>, 2025.
- Gariano, S. L. and Guzzetti, F.: Landslides in a changing climate, *Earth-Science Reviews*, 162, 227–252, <https://doi.org/https://doi.org/10.1016/j.earscirev.2016.08.011>, 2016.
- Gu, A. and Dao, T.: Mamba: Linear-Time Sequence Modeling with Selective State Spaces, <https://arxiv.org/abs/2312.00752>, 2024.
- Han, X., Zhang, X., Wu, Y., Zhang, Z., and Wu, Z.: KAN4TSF: Are KAN and KAN-based models Effective for Time Series Forecasting?, <https://arxiv.org/abs/2408.11306>, 2024.
- Huffman, G. J., Bolvin, D. T., Braithwaite, D., Hsu, K., Joyce, R., Xie, P., and Yoo, S.-H.: NASA global precipitation measurement (GPM) integrated multi-satellite retrievals for GPM (IMERG), Algorithm theoretical basis document (ATBD) version, 4, 30, 2015.
- Jemec Auflič, M., Bezak, N., Šegina, E., Frantar, P., Gariano, S. L., Medved, A., and Peternel, T.: Climate change increases the number of landslides at the juncture of the Alpine, Pannonian and Mediterranean regions, *Scientific Reports*, 13, 23 085, <https://doi.org/10.1038/s41598-023-50314-x>, 2023.
- Liu, Z., Wang, Y., Vaidya, S., Ruehle, F., Halverson, J., Soljačić, M., Hou, T. Y., and Tegmark, M.: KAN: Kolmogorov-Arnold Networks, <https://arxiv.org/abs/2404.19756>, 2024.
- Lundberg, S. and Lee, S.-I.: A Unified Approach to Interpreting Model Predictions, <https://arxiv.org/abs/1705.07874>, 2017.



- Mondini, A. C., Guzzetti, F., and Melillo, M.: Deep learning forecast of rainfall-induced shallow landslides, *Nature Communications*, 14, 2466, <https://doi.org/10.1038/s41467-023-38135-y>, 2023.
- 275 Nocentini, N., Rosi, A., Segoni, S., and Fanti, R.: Towards landslide space-time forecasting through machine learning: the influence of rainfall parameters and model setting, *Frontiers in Earth Science*, 11, <https://doi.org/10.3389/feart.2023.1152130>, 2023.
- Piciullo, L., Gariano, S. L., Melillo, M., Brunetti, M. T., Peruccacci, S., Guzzetti, F., and Calvello, M.: Definition and performance of a threshold-based regional early warning model for rainfall-induced landslides, *Landslides*, 14, 995–1008, <https://doi.org/10.1007/s10346-016-0750-2>, 2017.
- 280 Rosi, A.: Exploring the Use of Pattern Classification Approaches for the Recognition of Landslide-Triggering Rainfalls, *Sustainability*, 15, <https://doi.org/10.3390/su152015145>, 2023.
- Rosi, A., Segoni, S., Canavesi, V., Monni, A., Gallucci, A., and Casagli, N.: Definition of 3D rainfall thresholds to increase operative landslide early warning system performances, *Landslides*, 18, 1045–1057, <https://doi.org/10.1007/s10346-020-01523-2>, 2021.
- Segoni, S., Piciullo, L., and Gariano, S. L.: A review of the recent literature on rainfall thresholds for landslide occurrence, *Landslides*, 15, 1483–1501, <https://doi.org/10.1007/s10346-018-0966-4>, 2018a.
- 285 Segoni, S., Rosi, A., Lagomarsino, D., Fanti, R., and Casagli, N.: Brief communication: Using averaged soil moisture estimates to improve the performances of a regional-scale landslide early warning system, *Natural Hazards and Earth System Sciences*, 18, 807–812, <https://doi.org/10.5194/nhess-18-807-2018>, 2018b.
- Segoni, S., Nocentini, N., Barbadori, F., Medici, C., Gatto, A., Rosi, A., and Casagli, N.: A novel prototype national-scale landslide nowcasting system for Italy combining rainfall thresholds and risk indicators, *Landslides*, <https://doi.org/10.1007/s10346-024-02452-0>, 2025.
- 290 Tehrani, F. S., Calvello, M., Liu, Z., Zhang, L., and Lacasse, S.: Machine learning and landslide studies: recent advances and applications, *Natural Hazards*, 114, 1197–1245, <https://doi.org/10.1007/s11069-022-05423-7>, 2022.
- Wen, H., Yan, F., Huang, J., and Li, Y.: Interpretable machine learning models and decision-making mechanisms for landslide hazard assessment under different rainfall conditions, *Expert Systems with Applications*, 270, 126582, <https://doi.org/https://doi.org/10.1016/j.eswa.2025.126582>, 2025.
- 295 Xu, K., Chen, L., and Wang, S.: Kolmogorov-Arnold Networks for Time Series: Bridging Predictive Power and Interpretability, <https://arxiv.org/abs/2406.02496>, 2024.
- Zhang, J., Fan, Y., Cai, K., and Wang, K.: Kolmogorov-Arnold Fourier Networks, <https://arxiv.org/abs/2502.06018>, 2025.
- Zhang, Y. and Yan, J.: Crossformer: Transformer Utilizing Cross-Dimension Dependency for Multivariate Time Series Forecasting, in: *The Eleventh International Conference on Learning Representations*, <https://openreview.net/forum?id=vSVLM2j9eie>, 2023.
- 300 Zhao, K., Qiu, H., Liu, Y., Liu, Z., Huangfu, W., Tang, B., Yang, D., and Yang, G.: Probability of rainfall-induced landslides coupled with effective-duration threshold and soil moisture, *Journal of Hydrology: Regional Studies*, 57, 102112, <https://doi.org/https://doi.org/10.1016/j.ejrh.2024.102112>, 2025.